ORIGINAL ARTICLE

Molecules in cavity

Modified explicitly-correlated Fock-space coupled-cluster method for modeling confined molecular systems.

Aleksandr S. Bedniakov[1] | Denis Bokhan[1,2] | Dmitrii N. Trubnikov[1] | Yulia V. Novakovskaya[1]

[1]Department of Chemistry, Lomonosov Moscow State University, Moscow, 119991, Russian Federation

[2]Quantum Information Technologies Group, Russian Quantum Center, Skolkovo Innovation Center, Moscow, Russian Federation, 121205

Correspondence
Aleksandr S. Bedniakov, Department of Chemistry, Lomonosov Moscow State University, Moscow, 119991, Russian Federation
Email: BedniakovAS@my.msu.ru

Funding information
This work was supported partly by the Center of Laser Technologies and Materials Science (CLTM).

A model for calculation of the ground and excited state energies, single and double electron affinities and ionization potentials of a many-electron system confined in a cavity with a finite boundary potential is presented. Additional integrals of explicitly-correlated Fock-space coupled-cluster method are calculated numerically with the use of conventional Gaussian basis sets on the same type of fine grids as those used for one-electron integrals, which represents a rational and efficient tool for modeling confined systems. The method is verified by an example of H, He and LiH systems with spherical potential and applied to describing a representative set of diverse spin and orbital states of O_2 molecule and its ions. As the size of the system and so the total number of the basis functions are increased, the accuracy of predictions also increases. In the case of O_2 the internuclear distance is shown to be shortened with the increase in the potential wall height, while the energy differences between ${}^3\Sigma_g^-$, ${}^1\Delta_g$ and ${}^1\Sigma_g^+$ states change only slightly. Critical cavity radii are determined, which correspond to the spontaneous ionization of O_2 and the loss of an excess electron by O_2^-.

1 | INTRODUCTION

In the last decades an interest to the states of atoms and molecules in cavities of different shapes as the models of systems affected by a high pressure has steadily increased. These may be impurities in bulk and confined semiconductors [1, 2], inclusion compounds in matrices and fullerene-like cages [3] or in the stars [4]. A cavity can have an infinitely high potential wall (impenetrable) or a finite height wall (penetrable). It is interesting to note that the attractive forces between particles, such as van der Waals forces, can be modeled only with a finite potential. For single-electron systems, formal exact solutions for an impenetrable wall are obtained for different states in the form of confluent hypergeometric functions expressed as infinite sums, which become finite only in the case of a free atom [5, 6, 7]. In a cavity, the 2p-orbital energy of a hydrogen atom may become lower than that of 2s orbital. For either orbital, it is possible to find a critical radius of the cavity, when the binding energy vanishes [6].

Approximate solutions such as perturbation theory expansions, when the Coulomb potential is treated as a perturbation [8, 9, 10], or various kinds of variational approaches with [11] or without [12, 13, 14] special boundary conditions imposed on wave functions are also used. Such methods are suitable also for many-electron systems such as helium or other small atoms.

The problem of small atoms in a penetrable cavity has also been studied thoroughly [15, 16]. As the box radius is reduced, the energy was found to grow monotonously. In the case of boxes with impenetrable potential walls there is no upper limit for the orbital energy growth. In the case of penetrable walls, the upper limit is the barrier height, when ionization can take place [17]. Penetrable potential is always set as

$$\begin{cases} U(r) & r \in \Omega, \\ U_0 & r \in \Omega', \end{cases} \tag{1}$$

where Ω and Ω' are the interior and exterior regions of the cavity; $\mathrm{U}(r)$ is the Coulomb potential within the cavity and U_0 is the height of the confining potential. It this case the Coulomb potential outside the cavity is set to zero, which enables one to obtain analytical solutions for the hydrogen atom and facilitates the application of boundary conditions for many-electron atoms, but changes the whole problem. For example, the energy of the system with $\mathrm{U}_0 = 0$ differs from the energy of a free atom and depends on the radius of the box. For these reasons, we constructed a model where the Coulomb contribution to the potential energy both inside and outside the cavity is taken into account.

For many-electron atoms, it is typical to use the Roothaan-Hartree-Fock approach with modified Slater-type wave functions, taking into account the boundary conditions or using cut-off functions [18, 19, 20, 21]. HF method, however, essentially neglects the correlation effects, which results in a difference even for a free helium atom of about 0.04 Hartree as compared to the results of CI or other variational methods with multi-configuration wave functions [22, 23, 24]. The contribution of the correlation energy increases with a decrease in the cavity size, but begins to decrease at very small box radii [25]. The contribution of the electron correlation changes little for a helium atom (0.04 Hartree in the absence and on the average 0.05 Hartree in the presence of a confining cavity with an effective size close to the van der Waals radius), but increases for larger atoms. For Be^{2+} the electron correlation energy is by half larger. It can be expected that for larger atoms the difference can be more significant, and the more so for molecular systems. The use of modified Slater orbitals, despite their correct limiting behaviour, is accompanied by computational difficulties and, hence, is limited to small-size systems. In Ref.[26] a Gaussian basis set was used for solving the cavity problem. Conventional sets of Gaussian functions are more contracted in comparison with the Slater ones, and hence they are less sensitive to the variations in the cavity radius at very large or very small values. In such circumstances, the use of conventional basic sets can be difficult due to changes in the character of the wave function, when the external potential is present.The use of explicitly correlated calculations can partially fix this problem. Nevertheless, they provide a fairly good approximation for the cavities of a moderate size that are typical of chemical problems [26]. Furthermore, there are grounds to expect that for the basis sets larger than 6-311G or for polyatomic molecular systems described with a larger number of basis functions, Gaussian sets could provide a comparatively better approximation. The use of Gaussian functions substantially facilitates the numerical procedure, especially the calculation of two-electron integrals. Another important feature of Gaussian basis sets is the possibility to use conventional serial quantum chemistry calculations instead of the use of rather complex computational procedures with specially constructed bases. This work is the first application of explicitly-correlated Fock-space coupled-cluster method to systems in a cavity, in particular when considering doubly ionized systems. When solving the cavity problems, a proper selection of the basis set is one of the key problems. An indicator that a particular basis set is poor can be a non-monotonous behaviour of the total energy with the decrease in the cavity radius. However, it is not a necessary condition for some core orbitals [19]. Another sign is related to the natural effect of the increase in energy of the system with the growth of the potential barrier. When it is not the case, like in Ref.[16] where the energy of a helium atom in the cavity with $R > 2$ Bohr was higher at $U = 10$ a.u. than at $U = \infty$, it may again indicate a poor basic set quality. In this work we tried to use all the advantages of the Gaussian basic sets, making it possible to apply well-developed methods for calculating excited state energies, the first and second ionization potentials and single and double electron affinities of molecules [27]. At the same time, the explicitly correlated approach we use makes it possible to deal with incomplete basis sets, which may be especially important in the case of cavities when correlation effects become substantial.

The systems studied in this work include H, He and LiH diatomic particle, as well as O_2 molecule along with its ions. The former three systems were taken as reference examples to compare the results to those of other well-known methods. O_2 and its ions were investigated due to their importance in the chemistry of solids and solutions. In what concerns the cavity shape, we focused the study on spherical cavities as representing the most uniform effects of the compressed environments.

Thus, there are two main objects of the study, namely, on one hand, to obtain quantitative description of diverse electronic states of a particular molecule in cavity of a varying size and, on the other, to clarify the possibility of doing this with the use of an explicitly correlated method in combination with moderately flexible and relatively compact Gaussian-type basis sets. Both aspects are novel to the field and, hence, can shed light on the capability of quantum chemical approaches in solving unconventional problems. In Section 2 an overview of the methods used is given. We start with the Hartree-Fock model for a system in a penetrable cavity in Subsection 2.1 and continue with explicitly-correlated Fock-space coupled-cluster singles and doubles method in Subsections 2.2-2.4. In Subsection 2.5 some features of basis sets in view of the cavity problem are touched upon. Section 3 contains results for test systems, as well as for O_2 and O_2^- particles. Conclusions are formulated in Section 4.

2 | THEORY

Henceforth, i,j, $\ldots$, a,b, $\ldots$, $\alpha, \beta, \ldots$, p,q,$\ldots$ symbols are used for the notation of occupied, virtual, virtual in the complete basis set and all possible orbitals, respectively. For the active occupied and active virtual orbitals n and e,f symbols are used, respectively. Slater determinants that correspond to configurations with one electron removed are denoted as Φ_n, Φ^b_{ji}, $\ldots$, while Φ^e, Φ^{ba}_j, $\ldots$ stand for those that represent configurations with one extra electron. K variable enumerates nuclei.

2.1 | Hartree-Fock description of a system in a penetrable cavity

Let us start with the Hartree-Fock equations for a molecule in a cavity, where the total energy can be written as follows:

$$E_e = \sum_{i=1} \langle i|\hat{h}|i\rangle + \frac{1}{2}\sum_{i,j=1}(J_{ij} - K_{ij}), \tag{2}$$

$$\hat{h} = -\frac{1}{2}\nabla^2 - \sum_K \frac{Z_K}{r_K} + U(r), \tag{3}$$

$$U(r) = \begin{cases} 0 & 0 \le r < R, \\ U_0 & R \le r < \infty, \end{cases} \tag{4}$$

where J_{ij} and K_{ij} are Coulomb and exchange integrals, Z_K is the charge of Kth nucleus, r_K is the distance between an electron and this nucleus, R is the radius of the spherical cavity, U_0 is the height of the cavity wall. Here, the sole difference from the usual HF equations is the presence of the last term in $\hat{h}$. Additional $\langle i|U(r)|i\rangle$ one-electron integrals are calculated numerically on a fine grid. The atomic grids used for the calculation are constructed as 100-point radial and 302-point angular Lebedev-Laikov grids [28]. This scheme is the same as the one used for the calculation of many-electron integrals in explicitly-correlated methods.

2.2 | CCSD(F12) method for the ground state

Within the coupled-cluster (CC) theory, the ground-state wave function of a neutral system has the form

$$\Psi_0 = e^{(\hat{T}_1+\hat{T}_2+\ldots)}\Phi_0, \tag{5}$$

where $\hat{T}_n$ are regular cluster operators and Φ_0 is the ground-state Hartree-Fock determinant. The linearly approximated explicitly-correlated extension of the CC theory known as CC(F12) model [29] includes an additional operator, which takes care of the short-range correlation effects. In this work the coupled cluster singles and doubles (CCSD) ground state wave functions in the CCSD(F12) variant are used:

$$\Psi_{0,CCSD(F12)} = e^{(\hat{T}_1+\hat{T}_2+\hat{T}_2')}\Phi_0, \tag{6}$$

where the $\hat{T}_2'$ operator has the following form:

$$\hat{T}_2' = \frac{1}{2}\sum_{ijkl} t'^{ij}_{kl}\Big(\sum_{\alpha\beta}\langle\alpha\beta|f_{12}|kl\rangle\hat{E}_{\alpha i}\hat{E}_{\beta j} - \sum_{ab}\langle ab|f_{12}|kl\rangle\hat{E}_{ai}\hat{E}_{bj}\Big). \tag{7}$$

Here $\hat{E}_{pq}$ denotes a unitary group generator

$$\hat{E}_{pq} = a^+_{p\uparrow}a_{q\uparrow} + a^+_{p\downarrow}a_{q\downarrow}, \tag{8}$$

and f_{12} is a Slater-type geminal [30]:

$$f_{12} = -\frac{1}{\gamma}\exp(-\gamma r_{12}). \tag{9}$$

Geminal amplitudes are defined according to the Kato cusp conditions [31]:

$$t'^{ij}_{ij} = \frac{3}{8}, t'^{ij}_{ji} = \frac{1}{8}, t'^{ii}_{ii} = \frac{1}{2}, \tag{10}$$

while all the residual t'^{ij}_{kl} amplitudes are set to zero. Insofar as among the particles of interest, there are molecules and ions not only in singlet, but also in doublet and triplet either ground or excited states one of the ways to find the unknown energies is to use the equation-of-motion (EOM) scheme in combination with the estimation of ionization potentials (IP) and/or electron affinities (EA).

2.3 | EOM-CCSD(F12) methods

The IP-EOM-CCSD(F12) wave function of the target positively ionized state has the following form:

$$\Psi_{ion} = \hat{R}^{-}|\Psi_{0,CCSD(F12)}>, \tag{11}$$

where

$$\begin{aligned} \hat{R}^{-} &= \hat{R}_1^{-} + \hat{R}_2^{-} & (12)\\ \hat{R}_1^{-} &= \sum_i r_i a_i & (13)\\ \hat{R}_2^{-} &= \frac{1}{2}\sum_{i,j,a} r^a_{ij}\{a^{\dagger}_a a_i a_j\} & (14)\end{aligned}$$

and $\Psi_{0,CCSD(F12)}$ stands for the CCSD(F12) closed-shell wave function. With the use of $\bar{H} = e^{-T}\hat{H}e^{T}$ effective Hamiltonian, the IP-EOM-CCSD(F12) equations can be written in terms of projections onto the corresponding excitation manifold:

$$< \Phi_i|[\bar{H}, \hat{R}(n)^{-}]|\Phi_0 >= \omega_n < \Phi_i|\hat{R}(n)^{-}|\Phi_0 >, \tag{15}$$

$$< \Phi^a_{ij}|[\bar{H}, \hat{R}(n)^{-}]|\Phi_0 >= \omega_n < \Phi^a_{ij}|\hat{R}(n)^{-}|\Phi_0 >, \tag{16}$$

where ω_n is the ionization potential that corresponds to the nth root. The explicitly correlated set of Eqns.(15) and (16) has the same form, where the $\bar{H}$ elements are augmented with the terms originating from geminals [32].

In the case of an electron attachment, the target wave function can be written as

$$\Psi_{ea} = \hat{R}^{+}|\Psi_{0,CCSD(F12)}>, \tag{17}$$

where

$$\begin{aligned}\hat{R}^{+} &= \hat{R}_1^{+} + \hat{R}_2^{+} + \hat{R}_2^{+\prime} && (18)\\ \hat{R}_1^{+} &= \sum_a r_a a_a^{\dagger} && (19)\\ \hat{R}_2^{+} &= \frac{1}{2}\sum_{a,b,i} r_{ba}^{i}\{a_a^{\dagger}a_b^{\dagger}a_i\} && (20)\end{aligned}$$

$$\begin{aligned}\hat{R}_2^{+\prime} = \;& \frac{1}{2}\sum_{i,j,c,d}(r_c)t_{id}^{\prime jc}\Big(\sum_{\alpha,\beta}\langle\alpha\beta|f_{12}|dj\rangle\{a_\alpha^{\dagger}a_\beta^{\dagger}a_i\} - \sum_{a,b}\langle ab|f_{12}|dj\rangle\{a_a^{\dagger}a_b^{\dagger}a_i\}\Big) + \\ & \frac{1}{2}\sum_{i,j,c,d}(r_c)t_{dj}^{\prime ic}\times\Big(\sum_{\alpha,\beta}\langle\alpha\beta|f_{12}|jd\rangle\{a_\alpha^{\dagger}a_\beta^{\dagger}a_i\} - \sum_{a,b}\langle ab|f_{12}|jd\rangle\{a_a^{\dagger}a_b^{\dagger}a_i\}\Big)\end{aligned}$$

while the geminal amplitudes are determined again by the cusp conditions:

$$t_{jb}^{\prime ia} = \frac{3}{8}\delta_{ij}\delta_{ab}, \quad t_{bj}^{\prime ia} = \frac{1}{8}\delta_{ij}\delta_{ab}. \tag{21}$$

EA-EOM-CCSD(F12) working equations are also written in terms of the projections onto the proper excitation manifolds:

$$< \Phi^{a}|[\bar{H}, \hat{R}(n)^{+}]|\Phi_0 >= \omega_n < \Phi^{a}|\hat{R}(n)^{+}|\Phi_0 >, \tag{22}$$

$$< \Phi_i^{ba}|[\bar{H}, \hat{R}(n)^{+}]|\Phi_0 >= \omega_n < \Phi_i^{ba}|\hat{R}(n)^{+}|\Phi_0 >, \tag{23}$$

where ω_n corresponds now to EAs.

2.4 | IH-FS-CCSD(F12) method and its implementation

In practice when the goal is to reproduce a certain part of the full spectrum of a molecular $\hat{H}$ Hamiltonian restricted to a relatively small model M space (with the corresponding $M_{\perp}$ orthogonal complement), $\hat{H}_{eff}$ effective Hamiltonian can be constructed as

$$\hat{H}_{eff} = \hat{P}\hat{H}\hat{\Omega}\hat{P}, \tag{24}$$

where $\hat{P}$ is the projection operator onto M, $\hat{Q}$ stands for the projector onto $M_{\perp}$ and $\hat{\Omega}$ is a wave operator, so that both $\hat{H}_{eff}$ and $\hat{\Omega}$ satisfy Bloch equation:

$$\hat{H}\hat{\Omega}\hat{P} = \hat{\Omega}\hat{P}\hat{H}\hat{\Omega}\hat{P} = \hat{\Omega}\hat{H}_{eff}\hat{P} \tag{25}$$

In the Fock-space (FS) formalism, the wave operator is defined in the exponential form:

$$\hat{\Omega} = e^{\hat{T}}\{e^{\tilde{S}}\}\hat{P} \tag{26}$$

(where braces denote a normal-ordered form of the $\tilde{S}$ operator), which provides a hierarchical structure of the coupled cluster solutions. This means that when the Fock space problem for the (k, l) sector is formulated, the cluster operator includes all the lower rank sectors:

$$\tilde{S}^{(k,l)} = \sum_{i=0}^{k} \sum_{j=0}^{l} \hat{S}^{(i,j)} \tag{27}$$

To be able to find energies of triplet and doublet states, one needs $\tilde{S}^{(1,1)}$, $\tilde{S}^{(0,2)}$ and $\tilde{S}^{(2,0)}$ operators, the construction of which is based on the lower-sector operators, namely $\hat{S}^{(0,1)}$ and $\hat{S}^{(1,0)}$:

$$\hat{S}^{(0,1)} = \hat{S}_1^{(0,1)} + \hat{S}_2^{(0,1)} = \sum_{i\prime,n} s_{i\prime}^{n} a_n^\dagger a_{i\prime} + \frac{1}{2} \sum_{i,j,n,a} s_{ij}^{na} \{a_a^\dagger a_n^\dagger a_j a_i\}, \tag{28}$$

$$\hat{S}^{(1,0)} = \bar{S}^{(1,0)} + \hat{S}^{(1,0)\prime} \tag{29}$$

where

$$\bar{S}^{(1,0)} = \hat{S}_1^{(1,0)} + \hat{S}_2^{(1,0)} = \sum_{a\prime,e} s_e^{a\prime} a_{a\prime}^\dagger a_e + \frac{1}{2} \sum_{e,j,a,b} s_{ej}^{ab} \{a_a^\dagger a_b^\dagger a_e a_j\}, \tag{30}$$

$$\begin{aligned} \hat{S}^{(1,0)\prime} \quad = \quad & \frac{1}{2} \sum_{i,j,e,f} t_{if}^{\prime je} \Big(\sum_{\alpha,\beta} \langle \alpha\beta | f_{12} | fj \rangle \{a_\alpha^\dagger a_\beta^\dagger a_e a_i\} - \sum_{a,b} \langle ab | f_{12} | fj \rangle \{a_a^\dagger a_b^\dagger a_e a_i\} \Big) + \\ & \frac{1}{2} \sum_{i,j,e,f} t_{ie}^{\prime fj} \times \Big(\sum_{\alpha,\beta} \langle \alpha\beta | f_{12} | jf \rangle \{a_\alpha^\dagger a_\beta^\dagger a_e a_i\} - \sum_{a,b} \langle ab | f_{12} | jf \rangle \{a_a^\dagger a_b^\dagger a_e a_i\} \Big). \end{aligned}$$

In eqs. (28) and (30), prime symbol means the exclusion of excitations, which correspond to active orbitals. Amplitudes of $\bar{S}^{(0,1)}$ and $\bar{S}^{(1,0)}$ operators are calculated using the IP/EA-EOM-CCSD(F12) eigenvectors. Relations between IP/EA-EOM-CCSD(F12) vectors and the corresponding $\bar{S}^{(0,1)}$ and $\bar{S}^{(1,0)}$ amplitudes are given in detail in Ref.[33].

To solve the problems, it is reasonable to define intermediate effective Hamiltonians (IH) denoted as $\hat{H}_{\mathcal{I}}$ below. The use of $\hat{H}_{\mathcal{I}}$ has two main advantages. First, it solves the intruder-state problem, so that the larger active spaces can be used, and, thus, more accurate results can be obtained. Second, for the construction of $\hat{H}_{\mathcal{I}}^{(1,1)}$, $\hat{H}_{\mathcal{I}}^{(0,2)}$ and $\hat{H}_{\mathcal{I}}^{(2,0)}$, only $\hat{S}^{(0,1)}$ and $\hat{S}^{(1,0)}$ are required, and there is no need in solving the Bloch equation. This brings a significant simplification into the FS-CCSD computational scheme. In order to construct a space where $\hat{H}_{\mathcal{I}}$ is defined (M_0), we take a direct sum of the M model space and a certain part of $M_\perp$; the latter being an intermediate subspace $M_{\mathcal{I}}$, even though $M_{\mathcal{I}}$ formally remains a part of $M_\perp$. Subspaces $M_{\mathcal{I}}^{(1,1)}$, $M_{\mathcal{I}}^{(0,2)}$ and $M_{\mathcal{I}}^{(2,0)}$ are defined by taking determinants of the same type as in the corresponding model spaces, but with the excitation indices that involve both active and inactive occupied/virtual orbitals (except for those which are already contained in the model space). This is equivalent to the definition of $M_{\mathcal{I}}$ spaces via the action of $\hat{S}^{(1,1)}$, $\hat{S}^{(0,2)}$ and $\hat{S}^{(2,0)}$ operators on M [34, 35, 36]. For each sector $\hat{H}_{\mathcal{I}}$ is defined in $M_0 = M \bigoplus M_{\mathcal{I}}$ space (with the corresponding $\hat{P}_0$ projector onto model space and $\hat{Q}_0$ projector onto orthogonal space):

$$\hat{H}_{\mathcal{I}} = \hat{P}_0 \hat{H}_{\mathcal{I}} \hat{P}_0 \tag{31}$$

and according to Meissner [37] can be written as

$$\hat{H}_I = \hat{P}_0 \bar{H} \hat{P}_0 + \hat{P}_0 \bar{H} \hat{Y} \hat{P}_0, \tag{32}$$

where $\hat{Y} = \hat{Q}_0 \hat{X} \hat{P}$ and $\hat{X} = \{e^{\tilde{S}} - 1\}\hat{P}$. For each sector, $\hat{Y}$ can be written in terms of the lower-sector operators. Expressions for $\hat{Y}$ with F12 contributions are given elsewhere [27]. In practice for building the $\hat{H}_I$ matrix, $\bar{H}$ matrix in M_0 space is constructed and then $\hat{P}_0 \bar{H} \hat{Y} \hat{P}$ dressing terms are added according to Eq.(32). Diagonalization of $\hat{H}_I$ provides a set of unknown eigenvalues. Numbers of active occupied and virtual orbitals for the systems considered are listed in Table 1. The IH-FS-CCSD(F12) methods for (1,1), (0,2) and (2,0) sectors were implemented in the ACES III quantum chemistry software package [38]. The underlying CCSD(F12) method uses the B-approximation [39]. The necessary Slater and Yukawa integrals are evaluated using the Rys quadrature technique [40]. Many-electron integrals are computed with the numerical quadratures using the Becke fuzzy cell method [41]. The atomic grids used for the calculation of many-electron integrals are constructed as 50-point radial grids and 194-point Lebedev-Laikov angular grids [28].

	U_0	N_{act}^{occ}	N_{act}^{virt}
Ne	5	3	9
LiH	1	1	3
O_2^{2+}	5		6
	7		4
	9		4
O_2^{2-}	5	6	

TABLE 1 Numbers of active occupied (N_{act}^{occ}) and virtual (N_{act}^{virt}) orbitals for different systems, used in IH-FS-CCSD calculations

2.5 | Basis set

In cavity problems with penetrable walls, two regions exist, namely, those inside and outside the cavity. Inside the cavity, the Schrödinger equation for a hydrogen atom looks like

$$\frac{d^2 R_{nl}(r)}{dr^2} + \frac{2}{r}\frac{dR_{nl}(r)}{dr} + \left(2E + \frac{2}{r} - \frac{l(l+1)}{r^2}\right) R_{nl}(r) = 0 \tag{33}$$

Upon substituting $\rho = 2r/n$, $R_{nl}(\rho) = \exp^{-\frac{1}{2}\rho} \rho^l F(n,l,\rho)$, $E = -1/2n^2$ one comes [6] to

$$\rho \frac{d^2 F(n,l,\rho)}{d\rho^2} + (2l + 2 - \rho)\frac{dF(n,l,\rho)}{d\rho} + (n - 1 - l)F(n,l,\rho) = 0. \tag{34}$$

The solution of this differential equation is a confluent hypergeometric function ${}_1F_1(l+1-n, 2l+2, \rho)$. For a wide range of R values, n is very close to integers [42], so that the ${}_1F_1$ functions are close to generalized Laguerre polynomials. The exception is the case of a hydrogen atom in a small cavity with radii ≈3 Bohr and smaller, when n begins to increase rapidly, making the $R_{nl}(\rho)$ to differ from ordinary solutions for a free atom. In the region outside the cavity, the equation looks like

$$\frac{d^2\tilde{R}_l(r)}{dr^2}+\frac{2}{r}\frac{d\tilde{R}_l(r)}{dr}+(2E-2U_0+\frac{2}{r}-\frac{l(l+1)}{r^2})\tilde{R}_l(r)=0. \tag{35}$$

Upon substituting $E-U_0=-1/2\tilde{n}^2$ and $\tilde{\rho}=2r/\tilde{n}$, one comes to the same kind of equation as Eq. (34):

$$\tilde{\rho}\frac{d^2\tilde{F}(\tilde{n},l,\tilde{\rho})}{d\tilde{\rho}^2}+(2l+2-\tilde{\rho})\frac{d\tilde{F}(\tilde{n},l,\tilde{\rho})}{d\tilde{\rho}}+(\tilde{n}-1-l)\tilde{F}(\tilde{n},l,\tilde{\rho})=0. \tag{36}$$

The differences are in $\tilde{n}, \tilde{\rho}$ and the asymptotic $\tilde{R}(r)\to 0$ behavior as $\tilde{\rho}\to\infty$. The wavefunction vanishes at the infinity only for integer $\tilde{n}$ values, which reduces $\tilde{F}(\tilde{n},l,\tilde{\rho})$ to polynomials of degree $\tilde{n}$ by giving again generalized Laguerre polynomials.

Therefore, for not very small radii of the cavity, in both regions the wavefunction is close in its form to a Slater-type orbital (STO) with a scaled variable. This differs from the case of a zero Coulomb potential outside the cavity, when the function involves the $\tilde{\rho}^{-l-1}$ multiplier instead of $\tilde{\rho}^l$. There is an important scaling theorem [43], which states that if $\sum c_i\psi_i^G(\alpha_i)$ is the Gaussian expansion of an STO with the exponent parameter equal to unity, the expansion of an STO with an arbitrary ξ value of the exponent power factor can be expressed as $\sum c_i\psi_i^G(\xi^2\alpha_i)$. In the case of atoms enclosed in a cavity the power factor of the exponential function is greater than that for the free system. HOMO orbitals have smaller power factors compared to those of the core ones and are affected more noticeably when the cavity radius decreases. The Gaussian functions with large exponent power factors are always present in standard basis sets. This fact enables us to believe that standard Gaussian type expansions can serve as proper basis sets for solving problems with a non-zero Coulomb potential outside the cavity, especially in the case of molecules when the total number of basis functions is large.

3 | RESULTS AND DISCUSSION

3.1 | Test systems

There is not as much atomic and molecular systems for numerical tests of penetrable spherical potential barriers to compare with [15, 19, 20, 44, 17, 45, 16]. Most of them are one or two-electron systems. In order to test explicitly-correlated methods, systems with electron-electron interactions should be considered. Results for the smallest He atom and comparisons are given in Table 2. It is the most difficult case for the method used since the number of Gaussian functions is not large, and the quality of the wave-function approximation is expected to be poor in the case of small-radius cavities. It is worth noting that the results are not fully comparable to those of Ref.[19] where the Coulomb term outside the cavity was absent. Nevertheless, for relatively large cavities (with a radius of 4-6 Bohr), the results of Hartree-Fock calculations are expectedly very close, since they don't differ much from those for the free system. At a radius of 2 Bohr, our HF energy is higher by 0.05 Hartree, although the absense of a Coulomb potential should lead to an increase in the electronic energy. This fact indicates a poor approximation of the wave function with the selected basis set in the case of small radii of the cavity which could be expected taking into account the aforementioned peculiarity of an accurate analytic solution for a hydrogen atom at the cavity radii of 3 Bohr and smaller. Furthermore, at this cavity size, the maxima of the radial distribution functions of diffuse s and p atomic orbitals are located already outside the cavity, so that the apparent number of the basis functions that can be

R	E(HF)	E(CCSD)	E(HF)[44]
0.5	6.6048	6.5644	4.2233
1.0	-0.2034	-0.2442	-1.1871
1.5	-2.1161	-2.1567	-2.3811
2.0	-2.6628	-2.7035	-2.7116
3.0	-2.8210	-2.8616	-2.8461
4.0	-2.8596	-2.9012	-2.8601
6.0	-2.8612	-2.9028	-2.8617

TABLE 2 Ground-state HF and CCSD(F12) energies (Hartree) of a He atom in a penetrable cavity with $U_0 = 10$ a.u. and R radius (Bohr) obtained with the d-aug-cc-pVTZ basis set

involved in the description of the electron density distribution becomes smaller. The correlation energy for a helium atom changes little with the potential box radius and is approximately 0.04 Hartree.

For a larger Ne atom, the number of basis functions is increased (46 instead of 23 for He in the augmented triple-zeta Dunning basis set), so does the quality of the approximation. For a radius of 2 Bohr or smaller (Table 3) the HF energy is lower than those without the Coulomb term outside the cavity [44], as one should expect. For larger radii, a difference of 0.015-0.03 Hartree between our HF results and those of Ref.[44] is chiefly predetermined by the basis set error. This error value has the same order as in the case of helium, despite the fact that a neon atom is much larger and the same radius of the cavity corresponds to its more substantial effect on the electronic state. An explanation can be related to the greater number of the basis functions with the angular momenta up to $l = 3$, which fall within the cavity (there is only one p function with an RDF maximum at 3.3 Bohr and one d function with and RDF maximum at 2.0 Bohr in the case of aug-cc-pVTZ basis set) and, as a consequence, a better description of the compressed system. The correlation energy again changes little with the cavity radius and is approximately 0.31-0.34 Hartree. The first and second ionization potentials change slightly with a decrease in the radius of the cavity from 10 to 3 Bohr. When the cavity radius reaches the van der Waals radius of the atom ($\approx$2.98 Bohr [46]) a rapid drop can be noticed. The negative IP value at R=1.5 Bohr obtained with a double-zeta basis and the positive estimate with a triple-zeta set indicate the insufficient number of relatively compact functions in the former case. The single and double electron affinities are negative at all the cavity radii and noticeably increase in the absolute value as the confinement becomes stronger. It is not surprising since the smaller the radius of the box the less diffuse the character of the electron density distribution in the anion can be, which is not an energetically favourable situation. In what concerns the first excited state energy, it is lower than the ionization potential only until the cavity radius is larger than or equal to 5 Bohr. Upon further compression, the electron detachment becomes preferable compared to the excitation.

LiH is a test molecular system, for which results with a Coulomb contribution outside the cavity can be found [47]. Bartkowiak et al. used a very flexible basis set composed of 256 correlated Gaussian functions in variational approach. Absolute error of the CCSD(F12) energy values for the ground state with the use of double and triple-zeta basis sets (Table 4) amounts to only 0.013 and 0.0043 Hartree respectively despite the drastically more compact basis set. The number of basis functions (23 and 46 on H and Li atoms) is increased compared to a Ne atom, and so does the quality of approximation. Another factor that affects the accuracy is the existence of two different centres of the basis functions, which provides a higher flexibility of the basis set. While R is large, IP and DIP change little, EA and DEA change more noticeably and by contrast to a Ne atom, this molecule can even attach and keep an excess electron

R	E(HF)	E(CCSD)	E(HF)[19]	IP	DIP	EA	DEA	EE
				aug-cc-pVDZ				
1.0	-119.5573	-119.8387	-112.6710	-38.73	-45.65	-143.05	-292.05	93.54
1.5	-125.9451	-126.2400	-124.3938	-4.77	17.77	-114.47	-246.02	87.15
2.0	-127.5190	-127.8279	-127.3952	10.19	43.76	-71.75	-157.84	63.36
3.0	-128.4489	-128.7706	-128.4837	20.82	62.00	-43.43	-97.39	44.73
5.0	-128.4947	-128.8208	-128.5468	21.72	63.16	-8.40	-24.82	19.90
10	-128.4963	-128.8234	-128.5470	21.82	63.21	-7.33	-21.12	19.08
				aug-cc-pVTZ				
1.0	-119.3768	-119.7672	-112.6710	-38.41	-46.14	-142.03	-289.45	93.36
1.5	-126.5587	-126.8689	-124.3938	1.52	29.23	-106.09	-231.07	84.04
2.0	-127.8369	-128.1543	-127.3952	11.80	47.53	-73.32	-161.66	65.81
3.0	-128.4540	-128.7922	-128.4837	20.16	60.86	-35.51	-81.39	38.37
5.0	-128.5327	-128.8767	-128.5468	21.60	62.93	-8.01	-23.70	19.86
10	-128.5333	-128.8777	-128.5470	21.64	62.94	-6.42	-18.14	18.27

TABLE 3 Ground-state HF and CCSD(F12) energies (Hartree) along with the IP, DIP, EA, DEA and EE values (eV) of a Ne atom in a penetrable cavity with $U_0 = 5$ a.u. and R radius (Bohr)

when the cavity size exceeds 12 Bohr (Table 4). Thus, the systems, for which an addition of an electron is energetically favourable, may retain this ability even being located in a cavity with not as small radius. DEA decreases from -1.85 for the free system to -8.02 eV in the cavity of R=8 Bohr when aug-cc-pVTZ basis set is used, which reflects the formally increased repulsion of the second excess electron. Additionally, the single electron excitation of LiH in a cavity results in the formation of a bound electronic state, the electron detachment requiring nearly twice as high energy.

Thus, on the whole, the use of Gaussian basis sets for solving the cavity problems is more relevant at the larger number of electrons in a system. The existence of several centers of basis functions also improves the result. Both factors provide a better flexibility of the basis set and the larger angular momentum values that can formally correspond to the resulting approximations of one-electron orbitals. Very large (much larger than a van der Waals radius of the most distant atom) and very small (close to or smaller than the radius of the external valence orbitals) cavities represent situations when the solutions may be approximated with a lower accuracy because of the insufficient number of basis functions contributing to the description of the system in these regions. Thus, one can expect that molecules placed in moderate-sized cavities can be described relatively well with standard Gaussian-type basis sets of a triple-zeta quality.

Common features of the test systems confined in cavities are the slight changes in their electronic energies and IP and DIP values when the cavity radius decreases from large values to those close to a sum of van der Waals radii of the atoms. At the smaller cavity sizes the energy, IP, and DIP changes become large, and even the ionization of a system can take place. At the same time, a significant decrease in EA and DEA values begins already at the large radii, so the properties of the system related to the electron attachment can change even in cavities with a radius much larger than van der Waals ones. The correlation energy remains almost unchanged within the broad range of cavity sizes.

R	CCSD(F12)	E[47]	IP	DIP	EA	DEA	EE
			aug-cc-pVDZ				
8	-8.056791	-8.069751	7.99	30.35	-1.06	-8.38	3.55
9	-8.057338	-8.070159	8.00	30.36	-0.66	-7.00	3.38
10	-8.057601	-8.070289	8.01	30.37	-0.37	-5.86	3.28
12	-8.057758	-8.070333	8.01	30.38	-0.05	-4.69	3.24
15	-8.057783	-8.070335	8.01	30.38	0.15	-3.96	3.29
20	-8.057798	-8.070336	8.01	30.38	0.24	-2.57	3.34
∞	-8.057809	-8.070336	8.01	30.38	0.30	-1.97	3.42
			aug-cc-pVTZ				
8	-8.065032	-8.069751	8.02	30.47	-0.99	-8.02	3.60
9	-8.065444	-8.070159	8.03	30.48	-0.53	-6.45	3.42
10	-8.065611	-8.070289	8.04	30.49	-0.26	-5.47	3.33
12	-8.065704	-8.070333	8.04	30.49	-0.01	-4.44	3.29
15	-8.065719	-8.070335	8.04	30.49	0.18	-3.40	3.35
20	-8.065722	-8.070336	8.04	30.49	0.25	-2.53	3.40
∞	-8.065723	-8.070336	8.04	30.49	0.29	-1.85	3.47

TABLE 4 Ground-state CCSD(F12) energies (Hartree), IP, DIP, EA, DEA and EE energies (eV) for LiH molecule in a penetrable cavity with U_0 = 1 a.u. and R radius (Bohr)

3.2 | Oxygen molecule and its ions

The dependences of the interatomic distance and the energy of the ground triplet and lowest excited singlet states of the oxygen molecule on the position and height of the potential wall are studied in detail. As a reference system for the CCSD(F12) calculations, O_2^{2+} dication was taken and the energies of the neutral molecule (its ground and two lowest excited states) were estimated as DEA values with the use of IH-FS-CCSD(F12) method.

A series of calculations for different cavity radii in a range of 2.6–10 Bohr and different heights of the potential wall (5, 7 and 9 a.u.) at either frozen or unfrozen positions of the nuclei were carried out. The total electronic energies of the triplet and singlet states depending on the radius of the cavity obtained at the frozen interatomic distance typical of the equilibrium configuration of the triplet molecule are listed in Table 5 and illustrated by the plots in Fig.1. The cavity significantly affects the energy of the system when its radius becomes only slightly larger than a doubled van der Waals radius of an oxygen atom. In the case of an oxygen molecule, the distance between the molecular centre of mass and an oxygen atom is 1.1 Bohr, the van der Waals radius being 2.84 Bohr [48], so that the effective molecular radius can be estimated as nearly 4 Bohr. As follows from the plots, 5 Bohr is the cavity radius, when the energy of the system begins to increase, and this increase becomes significant when the radius decreases to 4 Bohr and below. It is worth noting that the change in the height of the potential wall from 5 to 7 and 9 Hartree does not practically affect the threshold position of the wall, at which a pronounced onset of the energy increase takes place. As follows from Fig.1, the energies of $^3\Sigma_g^-$, $^1\Delta_g$ and $^1\Sigma_g^+$ states change negligibly and nearly symbasically as the cavity size is

	U_0=5 a.u.			U_0=7 a.u.			U_0=9 a.u.		
R	$^3\Sigma_g^-$	$^1\Delta_g$	$^1\Sigma_g^+$	$^3\Sigma_g^-$	$^1\Delta_g$	$^1\Sigma_g^+$	$^3\Sigma_g^-$	$^1\Delta_g$	$^1\Sigma_g^+$
2.6	-148.5639	1.03	1.95	-148.3140	1.05	1.97	-148.1204	1.06	1.99
2.7	-148.8814	1.01	1.90	-148.6806	1.01	1.92	-148.5247	1.02	1.93
2.8	-149.1286	0.99	1.88	-148.9652	0.99	1.88	-148.8382	0.99	1.89
2.9	-149.3462	0.98	1.86	-149.2159	0.98	1.86	-149.1147	0.98	1.86
3.0	-149.5074	0.97	1.84	-149.4011	0.96	1.84	-149.3189	0.96	1.83
3.2	-149.7388	0.96	1.82	-149.6654	0.95	1.82	-149.6091	0.95	1.81
3.4	-149.8881	0.96	1.81	-149.8333	0.96	1.81	-149.7906	0.95	1.81
3.6	-149.9838	0.96	1.81	-149.9422	0.96	1.82	-149.9087	0.96	1.82
3.8	-150.0593	0.92	1.75	-150.0281	0.96	1.80	-150.0021	0.96	1.81
4.0	-150.1129	0.94	1.77	-150.0902	0.95	1.77	-150.0708	0.96	1.79
4.2	-150.1468	0.93	1.74	-150.1296	0.93	1.74	-150.1145	0.94	1.76
4.4	-150.1773	0.91	1.71	-150.1667	0.91	1.70	-150.1570	0.92	1.72
4.6	-150.1934	0.89	1.66	-150.1860	0.90	1.68	-150.1793	0.90	1.69
4.8	-150.2076	0.88	1.64	-150.2037	0.89	1.65	-150.2001	0.89	1.66
5.0	-150.2118	0.88	1.64	-150.2089	0.88	1.64	-150.2063	0.88	1.65
6.0	-150.2223	0.87	1.61	-150.2222	0.87	1.62	-150.2221	0.87	1.62
7.0	-150.2228	0.85	1.61	-150.2228	0.86	1.60	-150.2228	0.86	1.63
8.0	-150.2229	0.86	1.62	-150.2228	0.86	1.61	-150.2228	0.86	1.61
9.0	-150.2229	0.86	1.61	-150.2229	0.86	1.60	-150.2228	0.86	1.60
10.0	-150.2230	0.86	1.61	-150.2229	0.86	1.60	-150.2229	0.86	1.60
∞	-150.2230	0.86	1.61	-150.2229	0.86	1.60	-150.2229	0.86	1.60

TABLE 5 Absolute energies of the ground $^3\Sigma_g^-$ state (Hartree) and relative energies of the excited $^1\Delta_g$ and $^1\Sigma_g^+$ states (eV) of O_2 molecule in a penetrable cavity with U_0 barrier (a.u.) and R radius (Bohr)

decreased from 10 to ~5.0 Bohr, so that the energy gaps between the states remain nearly unchanged. As the cavity is further contracted, the energy increase of all the states becomes more pronounced, which is quite natural since the most diffuse *p*-orbital can no longer contribute to the description of the electron density distribution, whereas at larger cavity sizes its contribution was comparable to that of the function with an RDF maximum of 1.2 Bohr. At still smaller cavity radii, in a range of 3.2 to 3.8 Bohr, the symbate character of the energy changes is slightly distorted when, at first, the most diffuse *s*- and *d*-functions and then next-to-most diffuse *p*-function fall out of the set of those that can be involved in the approximation of external orbitals substantial for the $^1\Delta_g$ and $^1\Sigma_g^+$ states and $^3\Sigma_g^-$ state, respectively. Nevertheless, these minor effects do not change the overall trend in the state energies to increase rapidly with the cavity contraction: the curvature of 0.5 a.u. at R of 3.8-4.2 Bohr becomes as high as ≈7 a.u. at 2.7 Bohr. The strong cavity effect promotes the inevitable contraction of the internuclear distance in O_2 molecule (Table 6). $R(O\text{-}O)_{equil}$ was found as the one that corresponds to the minimum of the potential energy without taking into

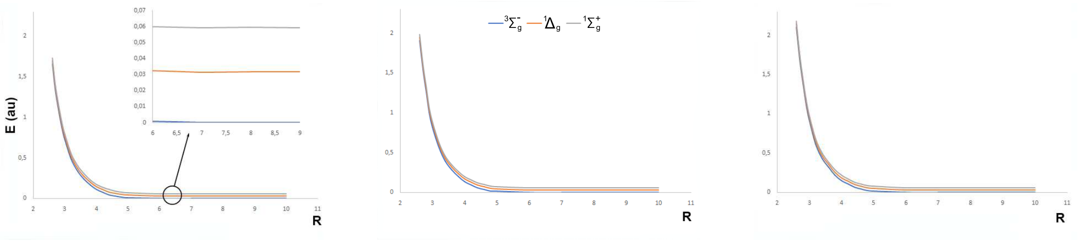

(a) U_0=5 a.u.

(b) U_0=7 a.u.

(c) U_0=9 a.u.

FIGURE 1 Energy dependence of the ground and two lowest excited states of O_2 molecule on the radius of the cavity (R, Bohr) and its wall height U_0.

account the zero oscillations. It can be noted again that in the cavities with a radius greater than 5 Bohr the equilibrium interatomic distance is almost unchanged. When the radius is further reduced, the rapid change in $R(O-O)$ begins and it reaches 2.08 Bohr at R=3.0 Bohr. Insofar as the neutral either triplet or singlet states of the oxygen molecule are rapidly destabilized in small cavities (with R less than 5 Bohr) and due to the double cation reference state used in the CCSD(F12) simulations, it seemed reasonable to analyse the possible ionization of the molecule. As follows from Table 7, within small-sized cavities, O_2^+ cation has a lower energy compared to the ground triplet state of the molecule, which reflects the possible spontaneous ionization of oxygen. At U_0=7 and 9 a.u. the effect takes place at a cavity radius of R=2.6 Bohr and 2.7 Bohr respectively. Note also that there is naturally a transient situation, when

R	$R(O\text{-}O)_{equil}$
3.0	2.08
3.2	2.12
3.4	2.14
3.6	2.14
3.8	2.16
4.0	2.16
4.2	2.18
4.4	2.20
4.6	2.20
4.8	2.20
5.0	2.22
6.0	2.22
7.0	2.22
8.0	2.22

TABLE 6 Changes in the equilibrium O-O internuclear distance ($R(O\text{-}O)_{equil}$, Bohr) in O_2 molecule depending on the cavity radius (R, Bohr) at the potential wall height of $U_0 = 5$ a.u.

the cation energy is lower than the $^1\Delta_g$ state of the molecule, but still higher than the $^3\Sigma_g^-$ state energy. It is observed within narrow R ranges, about 0.1-0.2 a.u. larger than the aforementioned thresholds. To study the state of O_2^- anion in a cavity and to check the estimated values for a neutral O_2 molecule a series of CCSD(F12) calculations for O_2^{2-} dianion followed by the EOM-IP(F12) and IH-FS-CCSD(F12) simulations were carried out. It can be seen (Table 8) that the energy difference between the $^3\Sigma_g^-$ state of a neutral molecule and $^2\Pi$ state of the anion decreases with a decrease in the radius of the cavity. Thus, an oxygen anion can survive only in cavities with a radius no smaller than 5 Bohr when its internuclear distance is shortened by 0.1 Bohr compared to the free system. Hence, for all the systems, the confining cavity induces the inevitable shortening of the internuclear distances, which naturally provides a poorer opportunity for the electron density localization and the electronic states with more diffuse distributions become less stable.

U_0 / R	5 a.u.			7 a.u.			9 a.u.		
	E(O_2,$^3\Sigma_g^-$)	E(O_2,$^1\Delta_g$)	E(O_2^+,$^2\Pi_g$)	E(O_2,$^3\Sigma_g^-$)	E(O_2,$^1\Delta_g$)	E(O_2^+,$^2\Pi_g$)	E(O_2,$^3\Sigma_g^-$)	E(O_2,$^1\Delta_g$)	E(O_2^+,$^2\Pi_g$)
2.6	20.68	21.72	20.83	23.19	24.24	21.97	25.06	26.12	22.82
2.7	17.69	18.69	19.46	19.83	20.84	20.43	21.44	22.46	21.15
2.8	15.15	16.14	18.31	17.00	17.99	19.14	18.39	19.38	19.77
2.9	12.94	13.92	17.31	14.53	15.51	18.02	15.73	16.70	18.55
3.0	11.07	12.04	16.47	12.46	13.42	17.09	13.50	14.45	17.54
3.2	8.24	9.20	15.22	9.34	10.30	15.69	10.16	11.11	16.05
3.4	6.07	7.03	14.29	6.98	7.94	14.67	7.67	8.63	14.96
3.6	4.56	5.52	13.64	5.30	6.26	13.95	5.89	6.85	14.19
3.8	3.24	4.16	13.11	3.82	4.78	13.34	4.31	5.27	13.53
4.0	2.25	3.19	12.72	2.69	3.64	12.89	3.07	4.02	13.03
4.2	1.60	2.53	12.47	1.94	2.88	12.60	2.25	3.19	12.71
4.4	0.98	1.89	12.24	1.19	2.10	12.32	1.39	2.31	12.39
4.6	0.64	1.53	12.12	0.80	1.69	12.18	0.93	1.84	12.23
4.8	0.34	1.23	12.02	0.43	1.31	12.05	0.50	1.39	12.07
5.0	0.25	1.13	11.99	0.31	1.19	12.01	0.37	1.25	12.02
6.0	0.01	0.88	11.91	0.01	0.88	11.91	0.01	0.88	11.91
7.0	0.00	0.86	11.91	0.00	0.86	11.91	0.00	0.86	11.91

TABLE 7 Energies (eV) of the neutral $^3\Sigma_g^-$ and $^1\Delta_g$ states of O_2 molecule and $^2\Pi_g$ state of O_2^+ cation depending on the cavity radius R (Bohr) and the potential wall height U_0 at an internuclear distance R(O-O)=2.2 Bohr with respect to the energy of $^3\Sigma_g^-$ of a free O_2 molecule

4 | CONCLUSIONS

In this work the explicitly-correlated IH-FS-CCSD(F12) method is for the first time implemented for (1,1), (0,2) and (2,0) sectors for studying the states of particles in a penetrable cavity with the use of Gaussian-type basis sets. Numerical tests for He, Ne and LiH systems demonstrate the applicability of Gaussian expansions for average-sized cavities. The

Potential minima	R(O-O)	$^3\Sigma_g^-$	$^2\Pi_g$	EA
		Free system		
	2.2	-150.1954	-150.2059	0.01
R(O-O)$_{equil}$ (O$_2$)	2.3	-150.2003	-150.2264	0.03
	2.4	-150.1973	-150.2380	0.04
	2.5	-150.1891	-150.2431	0.07
R(O-O)$_{equil}$ (O_2^-)	2.6	-150.1774	-150.2433	0.07
	2.65	-150.1706	-150.2421	0.07
		R=5 Bohr		
	2.2	-150.2173	-150.1782	-0.04
R(O-O)$_{equil}$ (O$_2$)	2.3	-150.2196	-150.1991	-0.02
	2.4	-150.2142	-150.2093	-0.01
R(O-O)$_{equil}$ (O_2^-)	2.5	-150.2034	-150.2113	0.01
	2.6	-150.1891	-150.2077	0.02
		R=4 Bohr		
	2.1	-150.1135	-149.9671	-0.15
R(O-O)$_{equil}$ (O$_2$)	2.2	-150.1206	-149.9938	-0.13
	2.3	-150.1144	-150.0027	-0.11
	2.4	-150.1031	-150.0059	-0.10
	2.5	-150.0833	-149.9974	-0.09
	2.6	-150.0543	-149.9740	-0.08
		R=3 Bohr		
	1.9	-149.5735	-149.1318	-0.44
R(O-O)$_{equil}$ (O$_2$)	2.0	-149.5884	-149.1700	-0.42
	2.1	-149.5802	-149.1808	-0.40
	2.2	-149.5191	-149.1272	-0.39
	2.3	-149.4542	-149.0677	-0.39
	2.4	-149.4020	-149.0258	-0.38
	2.5	-149.2898	-148.9070	-0.38
	2.6	-149.2240	-148.8479	-0.38

TABLE 8 The energies (Hartree) of the ground $^3\Sigma_g^-$ state of O_2 molecule and $^2\Pi_g$ state of O_2^- anion and the electron affinity (EA, eV) depending on the internuclear R(O-O) distance (Bohr) in a penetrable cavity with $U_0 = 5$ a.u. and R radius (Bohr)

accuracy of predictions is improved at the larger number of electrons in a system in the presence of several centres of basis functions.

The use of Gaussian functions provides an advantage of the implementation simplicity of the correlated methods like CCSD, EOM and Fock-Space methods in their explicitly correlated form for the evaluation of single and double ionization potentials, single and double electron affinities, and excitation energies that on the whole cover nearly all the possible states of the particles of interest.

IP and DIP values change only slightly when the cavity radius decreases to about a van der Waals radius of the atoms. At smaller radii the change becomes significant and even the spontaneous ionization takes place. EA and DEA values change within the whole range of the cavity radii, even at those larger than van der Waals radii. At the same time, the correlation energy remains almost unchanged for all the studied cavity sizes.

In the case of a neutral O_2 molecule R=5 Bohr is a radius of the cavity, when the rapid change of the electronic energy begins and it is almost independent of the potential wall height. At U_0=5 a.u. the equilibrium internuclear distance remains almost unchanged at the cavity radius larger than 5 Bohr and decreases significantly when the cavity is further contracted. Spontaneous ionization should take place at a cavity radius of 2.6-2.7 Bohr depending on the height of the potential wall. O_2^- anion can survive only in the cavity with U_0 no higher than 5 a.u. at the radius larger than 5 Bohr.

Finally, explicitly-correlated IH-FS-CCSD(F12) method for (1,1), (0,2) and (2,0) sectors in combination with relatively compact Gaussian basis sets of even triple-zeta quality provides a reasonable and efficient alternative approach for describing the systems located in penetrable cavities, if one is interested in estimating IP, DIP, EA and DEA values for the systems confined in moderate-size cavities.

Acknowledgment

This work has been supported partly by the Center of Laser Technologies and Materials Science (CLTM). We also thank the University of Florida High-Performance Computing Center (UF HPC) for providing computational facilities.

Data availability statement

The data that supports the findings of this study are available within the article.

References

[1] W.Kohn, Solid State Phys., **1957**, 5, 257-320.

[2] G. Bastard, *Les Ulis, Les Editions de Physique* **1988**.

[3] J.-P. Connerade, V.K.Dolmatov, S.T.Manson, *J. Phys. B: At. Mol. Opt. Phys* **1999**, 32, 395-403.

[4] A. Michels, J. de Boer, A. Bijl, *Physica* **1937**, 4, 981-994.

[5] A.Sommerfeld, H.Welker, *Ann.Physik* **1938**, 5, 56.

[6] S.R. de Groot, C.A. ten Seldam, *Physica XII* **1946**, 669.

[7] J.M.Ferreyra, C.R.Proetto, *Am. J. Phys.* **2013**, 81, 860.

[8] R.B. Dingle, *Proc. Camb. Phil. Soc.* **1953**, 49, 103.

[9] E.P.Wigner, *Phys. Rev.* **1954**, 94, 77.

[10] V.C. Aguilera-Navarro, W.M. Kloet, A.H. Zimermann, *Rev. Brasil Fis.* **1971**, 1, 55.

[11] P.L. Goodfriend, *J. Phys. B: At. Mol. Opt. Phys.* **1990**, 23, 1373.

[12] N. Aquino, *J. Phys. A: Math. Gen.* **1997**, 30, 2403.

[13] J. Gorecki, W. Byers Brown, *J. Phys. B: At. Mol. Opt. Phys.* **1989**, 22, 2659.

[14] J.L. Marin, S.A. Cruz, *J. Phys. B: At. Mol. Opt. Phys.* **1991**, 24, 2899.

[15] E.Ley-Koo, S.Rubinstein, *J. Chem. Phys.* **1979**, 71, 351.

[16] J.L. Marin, S.A. Cruz, *J. Phys. B: At. Mol. Opt. Phys.* **1992**, 25, 4365.

[17] N.Aquino, *Adv. in Quant. Chem.* **2009**, 57, 123-167.

[18] E.V. Ludena, *J. Chem. Phys.* **1978**, 69, 1770.

[19] M.Rodriguez-Bautista, C.Díaz-García, A.M. Navarrete-López, R.Vargas, and J.Garza, *J. Chem. Phys* **2015**, 143, 034103.

[20] M.Rodriguez-Bautista, R.Vargas, N.Aquino, J.Garza, *Int. J. Quantum Chem.* 2017, e25571.

[21] J.Garza, J.M.Hernandez-Perez, J.-Z.Ramirez, R.Vargas, *J. Phys. B: At. Mol. Opt. Phys.* **2012**, 45, 015002.

[22] C.L.Perekis, *Phys. Rev.* **1958**, 112, 1649.

[23] E.V. Ludena, M.Gregory, *J. Chem. Phys.* **1979**, 71, 2235.

[24] C.Joslin, S.Goldman, *J. Phys. B: At. Mol. Opt. Phys.* **1992**, 25, 1965-1975.

[25] B.M. Gimarc, *J. Chem. Phys.* **1967**, 47, 5110.

[26] R.Rivelino, J.D.M.Vianna, *J. Phys. B: At. Mol. Opt. Phys.* **2001**, 34, L645-L650.

[27] D.Bokhan, A.S.Bednyakov et al., *J. Chem. Phys.* **2021**, 155, N.1, 014107-1-014107-14.

[28] V. I. Lebedev and D. N. Laikov, *Doklady Mathematics* **1999**, 59, 477.

[29] D. P. Tew, W. Klopper and C. Hättig, *Chem. Phys. Lett.* **2008**, 452, 326.

[30] S. Ten-no, *Chem. Phys. Lett.* **2004**, 398, 56.

[31] S Ten-no, *J. Chem. Phys.* **2004**, 121, 117.

[32] D. Bokhan and S. Ten-no, *J. Chem. Phys.* **2010**, 132, 021101.

[33] D. Bokhan, D.N. Trubnikov and R.J. Bartlett, *J. Chem. Phys.* **2015**, 143, 074111.

[34] M. Musiał and R. J. Bartlett, *J. Chem. Phys.* **2008**, 129, 044101.

[35] M. Musiał and R. J. Bartlett, *J. Chem. Phys.* **2011**, 135, 044121.

[36] M. Musiał, *J. Chem. Phys.* **2012**, 136, 134111.

[37] L. Meissner, *J. Chem. Phys.* **1998**, 108, 9227.

[38] ACES III, Parallel Implementation of Electronic Structure Energy, Gradient and Hessian Calculations, V. Lotrich, N. Flocke, M. Ponton, A. D. Yau, S. A. Perera, E. Deumens and R. J. Bartlett, *J. Chem. Phys.* **2008**, 128, 194104.

[39] D. Bokhan, S. Bernadotte and S. Ten-no, *Chem. Phys. Lett.* **2009**, 469, 214.

[40] T. Shiozaki, *Chem. Phys. Lett.* **2009**, 479, 160.

[41] A. D. Becke, *J. Chem. Phys.* **1987**, 88, 2547.

[42] D. Suryanarayana and J. A. Weil, *J. Chem. Phys.* **1976**, 64, 510.

[43] K.O-ohata, H.Taketa and S.Huzinaga, *J. Phys. Soc. Japan* **1966**, 21, 2306.

[44] C.Diaz-Garcia, S.A.Cruz, *Int. J. Quant. Chem.* **2008**, 108, 1572-1588.

[45] N. Aquino and A. Flores-Riveros, *Electronic Structure of Quantum Confined Atoms and Molecules*, Sen K. (eds). Springer, Cham **2014**.

[46] Manjeera Mantina, Adam C. Chamberlin, Rosendo Valero, Christopher J. Cramer, Donald G. Truhlar *J. Phys. Chem. A* **2009**, 113, 5806-5812.

[47] W.Bartkowiak, K.Strasburger, *J. Mol. Struc.* **2010**, 960, 93-97.

[48] A.Bondi, *J. Phys. Chem.* **1964**, 68, N3, 441-451.